

INFORMATION TO USERS

The most advanced technology has been used to photograph and reproduce this manuscript from the microfilm master. UMI films the text directly from the original or copy submitted. Thus, some thesis and dissertation copies are in typewriter face, while others may be from any type of computer printer.

The quality of this reproduction is dependent upon the quality of the copy submitted. Broken or indistinct print, colored or poor quality illustrations and photographs, print bleedthrough, substandard margins, and improper alignment can adversely affect reproduction.

In the unlikely event that the author did not send UMI a complete manuscript and there are missing pages, these will be noted. Also, if unauthorized copyright material had to be removed, a note will indicate the deletion.

Oversize materials (e.g., maps, drawings, charts) are reproduced by sectioning the original, beginning at the upper left-hand corner and continuing from left to right in equal sections with small overlaps. Each original is also photographed in one exposure and is included in reduced form at the back of the book.

Photographs included in the original manuscript have been reproduced xerographically in this copy. Higher quality 6" x 9" black and white photographic prints are available for any photographs or illustrations appearing in this copy for an additional charge. Contact UMI directly to order.

U·M·I

University Microfilms International
A Bell & Howell Information Company
300 North Zeeb Road, Ann Arbor, MI 48106-1346 USA
313 761-4700 800 521-0600



Order Number 9030563

Fracture estimation in anisotropic media

Hood, Julie Anne, Ph.D.

University of Hawaii, 1990

U·M·I
300 N. Zeeb Rd.
Ann Arbor, MI 48106



FRACTURE ESTIMATION IN ANISOTROPIC MEDIA

A DISSERTATION SUBMITTED TO THE GRADUATE DIVISION OF THE
UNIVERSITY OF HAWAII IN PARTIAL FULFILLMENT
OF THE REQUIREMENTS FOR THE DEGREE OF

DOCTOR OF PHILOSOPHY

IN GEOLOGY AND GEOPHYSICS

MAY 1990

By

Julie A. Hood

Dissertation Committee:

Gerard J. Fryer, Chairman

Eduard Berg

Frederick K. Duenebier

Roy H. Wilkens

Alexander Malahoff

Dennis W. Moore

ACKNOWLEDGEMENTS

First and foremost, I want to thank my mother Joan for her encouragement and support during the past eleven years of college. Michael Schoenberg inspired my dissertation research with his anisotropic enthusiasm and it became a reality through his gracious help and advice. I appreciate Gerard Fryer for his financial support (National Science Foundation under grant OCE-8711646) and for the trust that I could and would produce something useful; Ed Berg for sharing his wisdom and patience; all my committee for their help and cooperation; Neil Frazer for introducing me to Michael Schoenberg; and Francis Muir of Stanford University for providing many helpful comments. I never would have completed this program without the support and welcomed distractions of my wonderful friends: the L.I.P.S. Club women and my special mainland friends and family. An especially big mahalo to Jo Ann Sinton for her unbounded kindness and Patricia Berge for her pragmatism and goddess-like bitchiness. Bagus terima kasih untuk kesabaranmu dan pikiranmu yang manis terus-menus dari Wayan dan Ketut di Bali. Finally, extra-special thanks and hugs to Mary Wilkowski for all her laughter, love, and editorial assistance. To all future graduate students I offer Hood's Law:

Bedenke stets, dass man zu seinem Vorgesetzten nicht "!"@?*&#*@"!" sagt!

ABSTRACT

A heterogeneous mixture of isotropic elements may appear homogeneous and anisotropic when the scale of its fabric is smaller than the seismic wavelengths that measure it. This fabric can result from thin layering, aligned crystals, anisotropic background stress, aligned fractures, and/or oriented microcracks. Horizontal layering in sedimentary basins and the oceanic crust generates transverse isotropy, a hexagonal symmetry with a vertical symmetry axis, an extremely common form of anisotropy. The elastic properties of transversely isotropic media do not vary with azimuth. With the advent of multi-component seismometers and walk-around experiments, however, azimuthal variation is now frequently observed as well. This azimuthal anisotropy usually results from steeply dipping aligned fractures or microcracks. Realistic earth models must include all the significant constituent anisotropies of fracture systems and the backgrounds in which these fracture systems are embedded. The anisotropy increases in complexity as the number of different systems incorporated into the medium increases. Considering all possible combinations of constituents, a variety of anisotropies can result. For example, embedding a fracture system into an isotropic background can produce anisotropy with a symmetry as simple as hexagonal or as complex as triclinic. Analysis of either fractures or the background requires separating the two anisotropic effects otherwise they interfere. As long as there is at least one symmetry plane in fractured anisotropic media, the contribution of the fractures to the elastic modulus matrix of the background can be removed. The fracture properties can be evaluated by imposing the background symmetry constraints. Once the fracture compliances are obtained, the elastic properties of the unfractured background and the complexity of its symmetry can be determined.

TABLE OF CONTENTS

ACKNOWLEDGEMENTS	iii
ABSTRACT	iv
LIST OF FIGURES	vii
INTRODUCTION	1
CHAPTER I - ESTIMATION OF VERTICAL FRACTURING	
FROM MEASURED STIFFNESS MODULI	3
Background	3
Vertically Fractured, Horizontally Stratified Media	4
Extraction of Fracture Compliances	
from Measured Stiffness Moduli	11
The G-element of the orthorhombic medium	11
Removing a set of fractures with unknown	
fracture compliances	12
Evaluating the unknown fracture compliances	
and background moduli	14
Measurements Sufficient to Determine	
Orthorhombic Stiffness Moduli	15
Discussion	17
CHAPTER II - A SIMPLE METHOD FOR DECOMPOSING	
FRACTURE-INDUCED ANISOTROPY	19
Background	19
Revisiting the Schoenberg and Muir Calculus	20
The Fracture Model	24
Example Involving Vertical Fractures	26
Discussion	29

CHAPTER III - SEPARATING CONSTITUENTS IN COMPLEX

ANISOTROPIC MEDIA 30

 Background 30

 Modeling a Fractured Medium 31

 A Procedure for Extracting Fracture Compliances
 from Measured Moduli 35

 Discussion 38

CONCLUSIONS 39

APPENDIX 40

 Outline of the Schoenberg and Muir Calculus 40

REFERENCES 44

LIST OF FIGURES

Figure	Page
1.1 Transversely isotropic medium	5
1.2 Vertically fractured, horizontally stratified medium with x_1 normal to the fracture planes and x_2 along fracture strike	7
2.1 Vertical fractures in a layered medium	21
3.1 Geometry of the Monoclinic System:	
(a) General 3D fractured, layered medium	
(b) The vertical x_1 - x_3 plane shows ϕ as the fracture dip angle	
(c) Plan-view shows the fracture strike parallels the x_2 axis	32

INTRODUCTION

Fine-scale layering predominates in the Earth's crust. Two of its more common manifestations are sedimentary basins and regions of basaltic volcanism. When layers are substantially thinner than a seismic wavelength, their elastic response is anisotropic [*Postma*, 1955; *Backus*, 1962] and displays hexagonal symmetry with a symmetry axis perpendicular to the layering. After a rock mass is formed, it is subjected to regional stresses that tend to open microcracks normal to the minimum compressive stress [*Hubbert and Willis*, 1957; *Crampin*, 1985]. A system of aligned cracks will also induce an anisotropy. These crack systems are assumed to have created the frequently observed azimuthal variations in shear-wave travel times in continental studies [*Willis et al.*, 1986] and marine experiments [*Stephen*, 1985]. The resulting seismic response displays a compound anisotropy, with contributions from both the initial rock mass formation and the current stress field. Study of either the formational anisotropy or the anisotropy from stress-aligned microcracks requires a decomposition of the compound anisotropy into its individual elements.

A similar situation occurs in the oceanic crust. Horizontal layering of lava flows, breccia zones, and pillow units induces an anisotropy that is enhanced by horizontal fractures [*Fryer et al.*, 1990]. The horizontal fracturing almost certainly occurs at the time of crustal formation [*Newmark et al.*, 1985]. Uplift to form the rift valley further fractures the crust; this time the fractures are near vertical [*Stephen*, 1985]. Again, the resultant anisotropy is a composite with contributions from the original formation and the fracturing.

This work considers the problem of decomposing anisotropy into its individual components. Specifically, Chapter I examines transversely isotropic rock which has been subjected to vertical fracturing and shows how the fracture-induced azimuthal anisotropy can be separated from the original background anisotropy (transversely

isotropic is understood here to imply hexagonal symmetry with a vertical symmetry axis). A set of parallel fractures vertically embedded in a transversely isotropic medium can result in a fractured medium that is equivalent to a homogeneous orthorhombic medium for long wavelengths. Using the group calculus formulation for layered media developed by Schoenberg and Muir [1989], the effects of the individual constituents can be separated arithmetically after the properties of each constituent are transformed. An outline of this calculus is given in the appendix.

Seismic anisotropy is often defined in terms of stiffness moduli. If the anisotropy is at least partly caused by fractures, however, the use of compliances rather than stiffnesses may simplify calculations. In addition, by aligning the coordinate system of each fracture set with the coordinate system of the background medium, elastic properties of fractured media can be more easily calculated and the complicated group element transformation procedures utilized in Chapter I can be avoided. In particular, this use of compliances and appropriate coordinate rotations simplifies the decomposition of the effects of fractures from a given suite of elastic properties. Chapter II presents a simplified method to decompose fracture-induced anisotropy and offers an example in which the effects of fractures are removed from a material with orthorhombic symmetry.

When sedimentary formations are tilted or when the minimum compressive stress is not horizontal, fracturing at angles non-vertical to the layering renders the medium monoclinic. In Chapter III, the technique of separating the fracture-induced azimuthal anisotropy from the original background anisotropy in orthorhombic systems is expanded to include monoclinic systems.

CHAPTER I

ESTIMATION OF VERTICAL FRACTURING FROM MEASURED STIFFNESS MODULI

Background

Although the function that couples the separate effects of vertical fractures and horizontal fabric is complicated, Schoenberg and Muir [1989] have developed a calculus that greatly simplifies the combination of the effects of layering and fracturing. Each constituent in a finely layered medium and each set of fractures can be represented by separate elements in a transform domain. In that domain, elements can be combined using simple addition, assuming that there is no nonlinear interaction between constituent layers and/or fracture sets. The result is then transformed back to the physical domain to produce the elastic properties of the more complicated system. Conversely, many complex anisotropic media can be decomposed in the transform domain. Simple subtraction reveals the properties of the separate anisotropic constituents of the total system.

The first section of this chapter uses the Schoenberg and Muir calculus to show how embedding vertical fractures in a transversely isotropic background results in a constrained orthorhombic medium. Although general orthorhombic media require nine elastic constants, only eight independent parameters are required to define this system. The necessary components of the Schoenberg and Muir calculus are presented in the appendix.

The section beginning on page 11, the focus of this chapter, shows that once estimates of elastic moduli for a region are determined, the unknown effects of the fractures can be subtracted from the background medium. The unknown fracture compliances can then be determined by imposing the constraint that the background be transversely isotropic. After these fracture compliances are evaluated, the elastic stiffness moduli of the transversely isotropic background medium can be found.

A proposed scheme of measurements for estimating these moduli is outlined in the section entitled *Measurements Sufficient to Determine Orthorhombic Stiffness Moduli*. The symmetry planes can be determined by rotating the horizontal component data until there is a minimum of cross talk between cross-line and in-line data [Alford, 1986]. The slower of the two symmetry planes is normal to the fractures. The three mutually orthogonal symmetry planes are then fixed as the horizontal plane, the vertical plane parallel to the fracture planes, and the vertical plane normal to the fractures. The corresponding coordinate axes are the x_3 axis vertical, x_2 parallel to the fractures, and x_1 perpendicular to the fracture planes. Using compressional shear sources, the elastic moduli can be obtained by a series of downhole and cross-hole shots along the symmetry planes.

Vertically Fractured, Horizontally Stratified Media

Consider a transversely isotropic medium of density ρ with its symmetry axis along the vertical x_3 axis (Fig. 1.1). The 6×6 matrix of elastic moduli in condensed notation (see, for example, Auld [1973]), specified by subscript b for background, is

$$C_b = \begin{bmatrix} c_{11b} & c_{12b} & c_{13b} & 0 & 0 & 0 \\ c_{12b} & c_{11b} & c_{13b} & 0 & 0 & 0 \\ c_{13b} & c_{13b} & c_{33b} & 0 & 0 & 0 \\ 0 & 0 & 0 & c_{44b} & 0 & 0 \\ 0 & 0 & 0 & 0 & c_{44b} & 0 \\ 0 & 0 & 0 & 0 & 0 & c_{66b} \end{bmatrix} \quad (1)$$

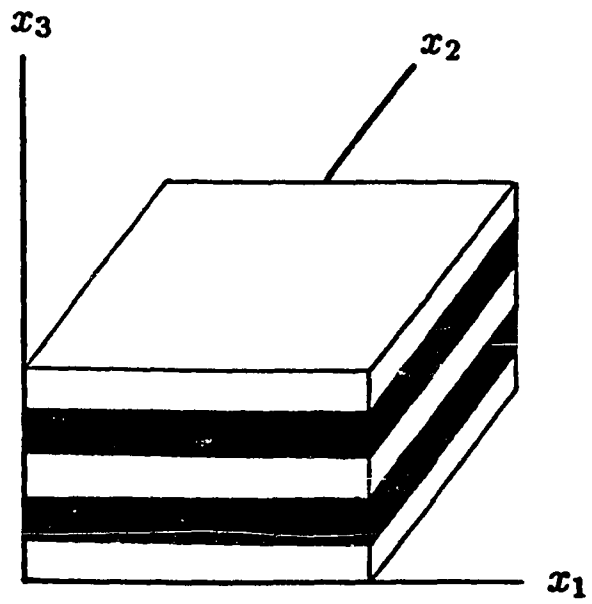


Figure 1.1 Transversely isotropic medium.

where

$$c_{12_b} = c_{11_b} - 2c_{66_b}. \quad (2)$$

Following the Schoenberg and Muir calculus outlined in the appendix, the 3×3 submatrices for \mathbf{C}_b relative to the x_1 direction are

$$\begin{aligned} \mathbf{C}_{NN_b} &= \begin{bmatrix} c_{11_b} & 0 & 0 \\ 0 & c_{44_b} & 0 \\ 0 & 0 & c_{66_b} \end{bmatrix}, \quad \mathbf{C}_{TN_b} = \begin{bmatrix} c_{12_b} & 0 & 0 \\ c_{13_b} & 0 & 0 \\ 0 & 0 & 0 \end{bmatrix}, \\ \mathbf{C}_{TT_b} &= \begin{bmatrix} c_{11_b} & c_{13_b} & 0 \\ c_{13_b} & c_{33_b} & 0 \\ 0 & 0 & c_{44_b} \end{bmatrix}. \end{aligned} \quad (3)$$

From (A6) in the appendix, the \mathbf{G} of a slab of thickness H (with the x_1 axis normal to the slab) in this transversely isotropic background medium is the 5-vector \mathbf{G}_b . The two scalar components and three 3×3 matrix components of \mathbf{G}_b are given by

$$\begin{aligned} g_b(1) &= H, \quad g_b(2) = H\rho, \\ \mathbf{g}_b(3) &= H \begin{bmatrix} \frac{1}{c_{11_b}} & 0 & 0 \\ 0 & \frac{1}{c_{44_b}} & 0 \\ 0 & 0 & \frac{1}{c_{66_b}} \end{bmatrix}, \quad \mathbf{g}_b(4) = \frac{H}{c_{11_b}} \begin{bmatrix} c_{12_b} & 0 & 0 \\ c_{13_b} & 0 & 0 \\ 0 & 0 & 0 \end{bmatrix}, \\ \mathbf{g}_b(5) &= H \begin{bmatrix} c_{11_b} - \frac{c_{12_b}^2}{c_{11_b}} & c_{13_b}(1 - \frac{c_{12_b}}{c_{11_b}}) & 0 \\ c_{13_b}(1 - \frac{c_{12_b}}{c_{11_b}}) & c_{33_b} - \frac{c_{13_b}^2}{c_{11_b}} & 0 \\ 0 & 0 & c_{44_b} \end{bmatrix}. \end{aligned} \quad (4)$$

Embedded in this medium is a set of large vertical fractures perpendicular to the x_1 direction (Fig. 1.2), modeled by parallel slip interfaces [Schoenberg, 1980]. The elastic behavior of these slip interfaces is specified by a 3×3 nonnegative definite fracture compliance matrix \mathbf{Z} . The matrix \mathbf{Z} reveals the slip of the fractures in a unit thickness as a linear function of the stress traction components acting across the fractures [Schoenberg and Douma, 1988]. This reference shows that parallel microcracks exhibit the same behavior. Corresponding to such a fracture set is a \mathbf{G} -element \mathbf{G}_f , whose

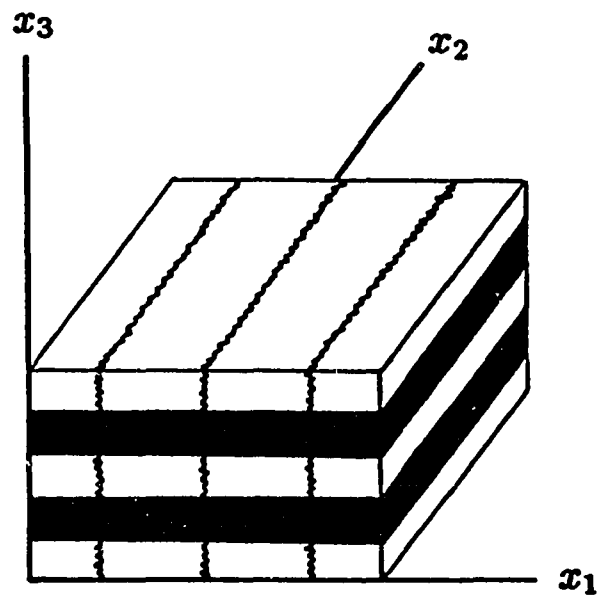


Figure 1.2 Vertically fractured, horizontally stratified medium with x_1 normal to the fracture planes and x_2 along fracture strike.

components are all zero except the third, $\mathbf{g}_f(3)$. The components of \mathbf{G}_f are given explicitly [Schoenberg and Muir, 1989] by

$$g_f(1) = 0, \quad g_f(2) = 0, \quad \mathbf{g}_f(3) = H\mathbf{Z}, \quad \mathbf{g}_f(4) = \mathbf{0}, \quad \mathbf{g}_f(5) = \mathbf{0}. \quad (5)$$

To retain orthorhombic symmetry in the fractured medium, the fractures themselves can be at most orthorhombic relative to the coordinate directions, x_1, x_2, x_3 . This causes \mathbf{Z} to be diagonal and its diagonal elements to be non-negative.

The physical significance of a diagonal \mathbf{Z} is that the compliance normal to the fractures, Z_N , is uncoupled from the tangential compliances, Z_3 and Z_2 . The tangential vertical compliance in the x_3 direction, Z_3 , is uncoupled from the tangential horizontal compliance in the x_2 direction, Z_2 . The compliance in these two directions need not be the same and the tangential slip need not be parallel to the tangential part of the stress traction. The fracture compliance matrix is written

$$\mathbf{Z} = \begin{bmatrix} Z_N & 0 & 0 \\ 0 & Z_3 & 0 \\ 0 & 0 & Z_2 \end{bmatrix} \quad (6)$$

where $Z_N, Z_3, Z_2 \geq 0$.

The \mathbf{G} of the vertically fractured transversely isotropic medium is found by simply adding the \mathbf{G} of the set of fractures to the \mathbf{G} of the background, i.e., $\mathbf{G} = \mathbf{G}_f + \mathbf{G}_b$. Since all components of \mathbf{G}_f are zero except the third, all components of \mathbf{G} are identical to those of \mathbf{G}_b as given by (4) except the third, $\mathbf{g}(3)$. Simple matrix addition gives $\mathbf{g}(3)$ as

$$\mathbf{g}(3) = H \begin{bmatrix} \frac{1}{c_{11b}} + Z_N & 0 & 0 \\ 0 & \frac{1}{c_{44b}} + Z_3 & 0 \\ 0 & 0 & \frac{1}{c_{66b}} + Z_2 \end{bmatrix}. \quad (7)$$

This \mathbf{G} -element satisfies constraints that specify the medium to be orthorhombic [Schoenberg and Muir, 1989], i.e., $\mathbf{g}(3)$ is diagonal, all elements of $\mathbf{g}(4)$ are zero except

the 1,1 and the 2,1 elements, and the 1,3 and 2,3 elements of $\mathbf{g}(5)$ are zero. The \mathbf{G} -element can be transformed back to physical medium parameters using (A7) of the appendix. This transformation leaves the density unchanged and gives the following 3×3 equivalent moduli submatrices:

$$\begin{aligned} \mathbf{C}_{NN} &= \begin{bmatrix} \frac{c_{11b}}{1+Z_N c_{11b}} & 0 & 0 \\ 0 & \frac{c_{44b}}{1+Z_3 c_{44b}} & 0 \\ 0 & 0 & \frac{c_{66b}}{1+Z_2 c_{66b}} \end{bmatrix}, \\ \mathbf{C}_{TN} &= \frac{1}{1+Z_N c_{11b}} \begin{bmatrix} c_{12b} & 0 & 0 \\ c_{13b} & 0 & 0 \\ 0 & 0 & 0 \end{bmatrix}, \\ \mathbf{C}_{TT} &= \begin{bmatrix} c_{11b} - \frac{Z_N c_{12b}^2}{1+Z_N c_{11b}} & c_{13b} - \frac{Z_N c_{12b} c_{13b}}{1+Z_N c_{11b}} & 0 \\ c_{13b} - \frac{Z_N c_{12b} c_{13b}}{1+Z_N c_{11b}} & c_{33b} - \frac{Z_N c_{13b}^2}{1+Z_N c_{11b}} & 0 \\ 0 & 0 & c_{44b} \end{bmatrix}. \end{aligned} \quad (8)$$

To simplify the representation of the 6×6 matrix of elastic moduli, the following dimensionless quantities are defined:

$$\delta_N = \frac{Z_N c_{11b}}{1+Z_N c_{11b}}, \quad \delta_3 = \frac{Z_3 c_{44b}}{1+Z_3 c_{44b}}, \quad \delta_2 = \frac{Z_2 c_{66b}}{1+Z_2 c_{66b}}. \quad (9)$$

Note that

$$0 \leq \delta_N, \delta_3, \delta_2 < 1. \quad (10)$$

These quantities relate the fracture compliance to the total compliance of the fractured medium: δ_N is that part of the total ϵ_1 resulting from the normal compliance of the fractures under the condition $\epsilon_2 = \epsilon_3 \equiv 0$; δ_3 is that part of the total ϵ_5 resulting from the vertical tangential compliance of the fractures, i.e., in the x_3 direction, with no restrictions on the other strain components; δ_2 is that part of the total ϵ_6 resulting from the horizontal tangential compliance of the fractures, i.e., in the x_2 direction, again, with no restrictions on the other strain components.

Combining the submatrices of equation (8) with definition (9) gives the 6×6 modulus matrix:

$$\mathbf{C} = \begin{bmatrix} c_{11} & c_{12} & c_{13} & 0 & 0 & 0 \\ c_{12} & c_{22} & c_{23} & 0 & 0 & 0 \\ c_{13} & c_{23} & c_{33} & 0 & 0 & 0 \\ 0 & 0 & 0 & c_{44} & 0 & 0 \\ 0 & 0 & 0 & 0 & c_{55} & 0 \\ 0 & 0 & 0 & 0 & 0 & c_{66} \end{bmatrix} \quad (11)$$

where

$$\begin{aligned} c_{11} &= c_{11_b}(1 - \delta_N), & c_{12} &= c_{12_b}(1 - \delta_N), \\ c_{13} &= c_{13_b}(1 - \delta_N), & c_{22} &= c_{11_b} \left(1 - \frac{\delta_N c_{12_b}^2}{c_{11_b}^2}\right), \\ c_{23} &= c_{13_b} \left(1 - \frac{\delta_N c_{12_b}}{c_{11_b}}\right), & c_{33} &= c_{33_b} \left(1 - \frac{\delta_N c_{13_b}^2}{c_{11_b} c_{33_b}}\right), \\ c_{44} &= c_{44_b}, & c_{55} &= c_{44_b}(1 - \delta_3), \\ c_{66} &= c_{66_b}(1 - \delta_2). \end{aligned}$$

The structure resulting from the much simpler case when the background is isotropic and the fractures are axisymmetric, i.e., $Z_2 = Z_3$, was discussed in detail by Schoenberg [1983]. The inequalities (10) imply that the absolute values of the moduli of the fractured medium are less than or equal to the corresponding moduli of the background transversely isotropic medium. The sole exception is $|c_{23}|$, which, if c_{12_b} is negative, increases with the addition of vertical fractures. In addition to the general stability conditions on orthorhombic media which result from \mathbf{c} being positive definite, (10) and (2) imply that

$$c_{55} \leq c_{44}, \quad c_{11} \leq c_{22}, \quad |c_{13}| \leq |c_{23}|. \quad (12)$$

Moreover, the relationship among some of the elements of \mathbf{c} ,

$$c_{22} = \frac{c_{23}}{c_{13}}(c_{11} + c_{12}) - c_{12}, \quad (13)$$

is easy to verify by direct substitution. For an orthorhombic medium with its azimuthal anisotropy caused by vertical fractures, this relation reduces the number of independent parameters from nine to eight.

Extraction of Fracture Compliances from Measured Stiffness Moduli

The previous section showed that adding a set of parallel vertical fractures (with at most orthorhombic symmetry relative to the coordinate axes) to a transversely isotropic background results in a medium with orthorhombic symmetry. This section begins with the orthorhombic elastic moduli of a vertically fractured rock mass where the x_1 axis is normal to the fractures. A three-step method evaluates the three fracture compliances of (6) associated with the vertical fractures and determines the elastic moduli of the transversely isotropic background without these fractures. The section beginning on page 15 presents an outline to measure the orthorhombic moduli and to find the orientation of the vertical fractures.

The G-element of the orthorhombic medium

The 6×6 elastic modulus matrix of an orthorhombic medium is of the form

$$\mathbf{C} = \begin{bmatrix} c_{11} & c_{12} & c_{13} & 0 & 0 & 0 \\ c_{12} & c_{22} & c_{23} & 0 & 0 & 0 \\ c_{13} & c_{23} & c_{33} & 0 & 0 & 0 \\ 0 & 0 & 0 & c_{44} & 0 & 0 \\ 0 & 0 & 0 & 0 & c_{55} & 0 \\ 0 & 0 & 0 & 0 & 0 & c_{66} \end{bmatrix}. \quad (14)$$

The assumption that these are the moduli for a vertically fractured transversely isotropic medium with the x_1 axis normal to the fractures implies that conditions (12) and (13) are satisfied. The submatrices of \mathbf{C} relative to x_1 are

$$\mathbf{C}_{NN} = \begin{bmatrix} c_{11} & 0 & 0 \\ 0 & c_{55} & 0 \\ 0 & 0 & c_{66} \end{bmatrix}, \quad \mathbf{C}_{TN} = \begin{bmatrix} c_{12} & 0 & 0 \\ c_{13} & 0 & 0 \\ 0 & 0 & 0 \end{bmatrix}, \quad \mathbf{C}_{TT} = \begin{bmatrix} c_{22} & c_{23} & 0 \\ c_{23} & c_{33} & 0 \\ 0 & 0 & c_{44} \end{bmatrix}. \quad (15)$$

A vertical slab (normal to the x_1 axis) of thickness H , density ρ , has the corresponding

\mathbf{G} -element, $\mathbf{G} = [g(1), g(2), g(3), g(4), g(5)]$, with components given by

$$\begin{aligned}
g(1) &= H, \quad g(2) = H\rho, \\
g(3) &= H \begin{bmatrix} \frac{1}{c_{11}} & 0 & 0 \\ 0 & \frac{1}{c_{55}} & 0 \\ 0 & 0 & \frac{1}{c_{66}} \end{bmatrix}, \quad g(4) = \frac{H}{c_{11}} \begin{bmatrix} c_{12} & 0 & 0 \\ c_{13} & 0 & 0 \\ 0 & 0 & 0 \end{bmatrix}, \\
g(5) &= H \begin{bmatrix} c_{22} - \frac{c_{12}^2}{c_{11}} & c_{23} - \frac{c_{12}c_{13}}{c_{11}} & 0 \\ c_{23} - \frac{c_{12}c_{13}}{c_{11}} & c_{33} - \frac{c_{13}^2}{c_{11}} & 0 \\ 0 & 0 & c_{44} \end{bmatrix}.
\end{aligned} \tag{16}$$

Removing a set of fractures with unknown fracture compliances

Using the Schoenberg and Muir calculus for decompositions, the removal of vertical fractures from the medium can be represented as

$$\text{Background Rock} = \text{Fractured Rock} - \text{Vertical Fractures}$$

or, using \mathbf{G} -elements $\mathbf{G}_b = \mathbf{G} - \mathbf{G}_f$, where \mathbf{G}_f and \mathbf{G}_b correspond to the set of fractures and the unfractured transversely isotropic background, respectively.

Since (5) shows that only the third component of the \mathbf{G} corresponding to a set of parallel fractures is non-zero, \mathbf{G} and \mathbf{G}_b are the same, except for the third component. Thus, removing an unknown set of fractures that is at most orthorhombic is equivalent to subtracting an unknown \mathbf{G}_f from \mathbf{G} where \mathbf{G}_f is of the form of (5), with Z given by (6). The \mathbf{G}_b in terms of the three unknown fracture compliances is

$$\begin{aligned}
g_b(1) &= H, \quad g_b(2) = H\rho, \\
g_b(3) &= H \begin{bmatrix} \frac{1}{c_{11}} - Z_N & 0 & 0 \\ 0 & \frac{1}{c_{55}} - Z_3 & 0 \\ 0 & 0 & \frac{1}{c_{66}} - Z_2 \end{bmatrix}, \quad g_b(4) = \frac{H}{c_{11}} \begin{bmatrix} c_{12} & 0 & 0 \\ c_{13} & 0 & 0 \\ 0 & 0 & 0 \end{bmatrix}, \\
g_b(5) &= H \begin{bmatrix} c_{22} - \frac{c_{12}^2}{c_{11}} & c_{23} - \frac{c_{12}c_{13}}{c_{11}} & 0 \\ c_{23} - \frac{c_{12}c_{13}}{c_{11}} & c_{33} - \frac{c_{13}^2}{c_{11}} & 0 \\ 0 & 0 & c_{44} \end{bmatrix}.
\end{aligned} \tag{17}$$

Using (A7) to transform back to physical parameters leaves the density unchanged.

The three 3×3 submatrices are

$$\begin{aligned} \mathbf{C}_{NN_b} &= \begin{bmatrix} \frac{c_{11}}{1-Z_N c_{11}} & 0 & 0 \\ 0 & \frac{c_{55}}{1-Z_3 c_{55}} & 0 \\ 0 & 0 & \frac{c_{66}}{1-Z_2 c_{66}} \end{bmatrix}, \\ \mathbf{C}_{TN_b} &= \frac{1}{1-Z_N c_{11}} \begin{bmatrix} c_{12} & 0 & 0 \\ c_{13} & 0 & 0 \\ 0 & 0 & 0 \end{bmatrix}, \\ \mathbf{C}_{TT_b} &= \begin{bmatrix} c_{22} + \frac{Z_N c_{12}^2}{1-Z_N c_{11}} & c_{23} + \frac{Z_N c_{12} c_{13}}{1-Z_N c_{11}} & 0 \\ c_{23} + \frac{Z_N c_{12} c_{13}}{1-Z_N c_{11}} & c_{33} + \frac{Z_N c_{13}^2}{1-Z_N c_{11}} & 0 \\ 0 & 0 & c_{44} \end{bmatrix}, \end{aligned} \quad (18)$$

defined in terms of the measured elastic moduli and the three unknown fracture parameters Z_N , Z_3 , and Z_2 .

For brevity, the dimensionless quantities E_N , E_3 , and E_2 are introduced:

$$E_N = \frac{Z_N c_{11}}{1 - Z_N c_{11}}, \quad E_3 = \frac{Z_3 c_{55}}{1 - Z_3 c_{55}}, \quad E_2 = \frac{Z_2 c_{66}}{1 - Z_2 c_{66}}. \quad (19)$$

Combining submatrices (18) allows the 6×6 matrix of elastic moduli to be written as

$$\mathbf{C}_b = \begin{bmatrix} c_{11_b} & c_{12_b} & c_{13_b} & 0 & 0 & 0 \\ c_{12_b} & c_{22_b} & c_{23_b} & 0 & 0 & 0 \\ c_{13_b} & c_{23_b} & c_{33_b} & 0 & 0 & 0 \\ 0 & 0 & 0 & c_{44_b} & 0 & 0 \\ 0 & 0 & 0 & 0 & c_{55_b} & 0 \\ 0 & 0 & 0 & 0 & 0 & c_{66_b} \end{bmatrix} \quad (20)$$

where

$$\begin{aligned} c_{11_b} &= c_{11}(1 + E_N), \quad c_{12_b} = c_{12}(1 + E_N), \\ c_{13_b} &= c_{13}(1 + E_N), \quad c_{22_b} = c_{22} + E_N \frac{c_{12}^2}{c_{11}}, \\ c_{23_b} &= c_{23} + E_N \frac{c_{12} c_{13}}{c_{11}}, \quad c_{33_b} = c_{33} + E_N \frac{c_{13}^2}{c_{11}}, \\ c_{44_b} &= c_{44}, \quad c_{55_b} = c_{55}(1 + E_3), \quad c_{66_b} = c_{66}(1 + E_2). \end{aligned}$$

Noting that $C_b - C$ is the same whether expressed in terms of measured moduli or background moduli, it is easy to show that

$$E_K = \frac{\delta_K}{1 - \delta_K}, \quad (21a)$$

or, conversely

$$\delta_K = \frac{E_K}{1 + E_K}, \quad K = N, 3, 2. \quad (21b)$$

So from (19)

$$\delta_N \equiv Z_N c_{11}, \quad \delta_3 \equiv Z_3 c_{55}, \quad \delta_2 \equiv Z_2 c_{66}, \quad (22)$$

and from (9)

$$E_N \equiv Z_N c_{11_b}, \quad E_3 \equiv Z_3 c_{55_b}, \quad E_2 = Z_2 c_{66_b}. \quad (23)$$

The E are the ratios of strain components in the fractures to corresponding strain components in the background, with the proviso, as in the discussion following (10) on the meaning of the δ , that E_N is the ratio of normal compliance in the fractures to ϵ_1 in the background when $\epsilon_2 = \epsilon_3 \equiv 0$.

Evaluating the unknown fracture compliances and background moduli

The unknown fracture compliances can be evaluated by satisfying the four conditions required for the background medium to be transversely isotropic:

$$(a) c_{44_b} = c_{55_b}, \quad (b) c_{13_b} = c_{23_b}, \quad (c) c_{11_b} = c_{22_b}, \quad (d) c_{12_b} = c_{11_b} - 2c_{66_b}.$$

Condition (a) on (20) gives

$$E_3 = \frac{c_{44}}{c_{55}} - 1 \equiv \frac{Z_3 c_{55}}{1 - Z_3 c_{55}} \quad (24)$$

or

$$Z_3 = \frac{1}{c_{55}} - \frac{1}{c_{44}}. \quad (25)$$

Conditions (b) and (c) on (20) give

$$\frac{c_{11}(c_{23} - c_{13})}{c_{13}(c_{11} - c_{12})} = E_N \equiv \frac{Z_N c_{11}}{1 - Z_N c_{11}} = \frac{c_{11}(c_{11} - c_{22})}{c_{12}^2 - c_{11}^2}. \quad (26)$$

Due to (13), which must hold if the measured parameters are made on a vertically fractured transversely isotropic medium, the two expressions for E_N are identical. Both yield

$$Z_N = \frac{c_{23} - c_{13}}{c_{11}c_{23} - c_{12}c_{13}}. \quad (27)$$

Condition (d) on (20) gives

$$E_2 = \frac{c_{11} - c_{12}}{2c_{66}}(1 + E_N) - 1 = \frac{c_{11}c_{23} - c_{12}c_{13}}{2c_{13}c_{66}} - 1 \equiv \frac{Z_2c_{66}}{1 - Z_2c_{66}} \quad (28)$$

or

$$Z_2 = \frac{1}{c_{66}} - \frac{2c_{13}}{c_{11}c_{23} - c_{12}c_{13}}. \quad (29)$$

This process reveals the three fracture compliances in terms of the measured parameters.

The dimensionless fracture parameters, E_N , E_3 , and E_2 , may then be substituted back into \mathbf{C}_b , (20), giving the unfractured transversely isotropic background moduli in terms of the measured c_{ij} . The 6×6 transversely isotropic elastic modulus matrix is

$$\mathbf{C}_b = \begin{bmatrix} c_{11_b} & c_{12_b} & c_{13_b} & 0 & 0 & 0 \\ c_{12_b} & c_{11_b} & c_{13_b} & 0 & 0 & 0 \\ c_{13_b} & c_{13_b} & c_{33_b} & 0 & 0 & 0 \\ 0 & 0 & 0 & c_{44_b} & 0 & 0 \\ 0 & 0 & 0 & 0 & c_{44_b} & 0 \\ 0 & 0 & 0 & 0 & 0 & \frac{c_{11_b} - c_{12_b}}{2} \end{bmatrix} \quad (30)$$

where the matrix elements are given by (20), completing the inversion for all the unknown parameters.

Measurements Sufficient to Determine Orthorhombic Stiffness Moduli

Substituting a plane wave of frequency ω and slowness components s_1, s_2, s_3 , i.e., $u_i = U_i \exp(s_j x_j - \omega t)$, into the displacement equations of motion gives the Christoffel equation

$$(c_{ijkl}s_k s_l - \rho \delta_{ji})U_i = 0. \quad (31)$$

The set of all real eigensolutions s_j of equation (31) is the slowness surface of an anisotropic elastic medium. An orthorhombic medium with three mutually perpendicular mirror symmetry planes aligned with the coordinate planes has an elastic modulus matrix, in condensed notation, of the form of (14). Substitution of (14) into (31) gives the Christoffel equations for orthorhombic media:

$$\begin{aligned}
(c_{11}s_1^2 + c_{66}s_2^2 + c_{55}s_3^2 - \rho)U_1 + (c_{12} + c_{66})s_1s_2U_2 + (c_{13} + c_{55})s_1s_3U_3 &= 0, \\
(c_{12} + c_{66})s_1s_2U_1 + (c_{66}s_1^2 + c_{22}s_2^2 + c_{44}s_3^2 - \rho)U_2 + (c_{23} + c_{44})s_2s_3U_3 &= 0, \\
(c_{13} + c_{55})s_1s_3U_1 + (c_{23} + c_{44})s_2s_3U_2 + (c_{55}s_1^2 + c_{44}s_2^2 + c_{33}s_3^2 - \rho)U_3 &= 0.
\end{aligned} \tag{32}$$

The three vertical slownesses give c_{33} , c_{44} and c_{55} by setting $s_1 = s_2 \equiv 0$ in (32); c_{44} is evaluated from the faster and c_{55} from the slower of the two shear waves. The x_1 and x_2 directions can be determined from the polarizations of these shear waves. The polarization of the faster gives the strike of the fractures, x_2 ; the polarization of the slower gives the normal to the fractures, x_1 . Alternatively, x_1 and x_2 can be determined from the orthogonal directions in which SH and SV waves propagate without shear-wave splitting. The faster of these directions is in the plane of the fractures; the slower is normal to the plane of the fractures.

For propagation in the x_1, x_3 plane normal to the fractures ($s_2 \equiv 0$), the use of (32) yields

$$\begin{aligned}
(c_{11}s_1^2 + c_{55}s_3^2 - \rho)U_1 + (c_{13} + c_{55})s_1s_3U_3 &= 0, \\
(c_{66}s_1^2 + c_{44}s_3^2 - \rho)U_2 &= 0, \\
(c_{13} + c_{55})s_1s_3U_1 + (c_{55}s_1^2 + c_{33}s_3^2 - \rho)U_3 &= 0.
\end{aligned} \tag{33}$$

Then c_{66} can be estimated from the slowness of a non-vertical SH wave using the uncoupled equation of (33); c_{11} and c_{13} can be estimated from the slownesses of two or more non-vertical in-plane waves (quasi- P and quasi- SV) using the coupled equations of (33).

For propagation in the x_2, x_3 plane parallel to the fractures ($s_1 \equiv 0$), the use of (32) yields

$$\begin{aligned} (c_{66}s_2^2 + c_{55}s_3^2 - \rho)U_1 &= 0, \\ (c_{22}s_2^2 + c_{44}s_3^2 - \rho)U_2 + (c_{23} + c_{44})s_2s_3U_3 &= 0, \\ (c_{23} + c_{44})s_2s_3U_2 + (c_{44}s_2^2 + c_{33}s_3^2 - \rho)U_3 &= 0, \end{aligned} \quad (34)$$

and c_{22} and c_{23} can be estimated from the slownesses of two or more non-vertical in-plane waves using the coupled equations of (34).

The measurements made in these vertical symmetry planes supply estimates for eight of the nine orthorhombic parameters; c_{12} remains to be determined. Estimating c_{12} requires a measurement out of the vertical coordinate planes as c_{12} appears in (32) multiplied by s_1s_2 . Once all nine parameters are estimated, the assumption that the medium consists of a transversely isotropic background with parallel vertical fractures can be verified by examining whether constraint (13) is satisfied.

Discussion

Once elastic moduli are obtained, the foregoing method can be used to determine whether the medium results from vertical fractures embedded in a transversely isotropic background. The interdependence between some of the elastic parameters (equation (13)) provides a basis for determining how closely the subject medium conforms to a vertically fractured transversely isotropic model. If it does, these calculations determine the relevant fracture compliances and the moduli of the background without vertical fractures. If the fracture behavior is axisymmetric, i.e., $Z_2 = Z_3$, then from (25) and (29), there is an additional relation on the measured c_{ij} which can easily be checked.

The Schoenberg and Muir calculus has been applied to derive explicit formulae for the fracture compliances and the background transversely isotropic elastic moduli as functions of the measured orthorhombic moduli of the long wavelength equivalent

medium. A remaining difficulty is to make a sufficiently accurate determination of these orthorhombic parameters in a reservoir or other subsurface region of interest.

CHAPTER II

A SIMPLE METHOD FOR DECOMPOSING FRACTURE-INDUCED ANISOTROPY

Background

Fractures are typically modeled through their effects on elastic stiffness moduli. Elastic compliances, however, can be estimated as readily as elastic stiffness moduli and their use substantially simplify calculations if the anisotropy is at least partly caused by fractures. In addition, any system of parallel fractures suggests an 'eigencoordinate' system (i.e., coordinate axes perpendicular and parallel to fracture planes). If the material properties of the resultant material are expressed in such coordinates further substantial simplifications can be made. In particular, this use of compliances and coordinate manipulations simplifies the separation of the effects of fractures from a given suite of elastic properties, and the complicated group element transformations of Schoenberg and Muir [1989] can be completely avoided.

Aligned flat ellipsoidal microcracks were first modeled by changes in the elastic stiffness matrix of material [Garbin and Knopoff, 1973, 1975; Hoenig, 1978, 1979; Hudson, 1980, 1981]. Schoenberg [1983] modeled the elastic response of fractured material using parallel slip interfaces and used compliances to specify the fracture properties. The parameters that characterized the change from virgin to fractured material were defined, however, relative to background stiffness moduli. Schoenberg

and Douma [1988] extended this concept to all physically possible fracture systems and modeled the resulting anisotropies. Schoenberg and Muir [1989] used matrix and group theory to calculate long wavelength equivalent properties for complex multi-constituent systems but still in terms of stiffness moduli. Using the Schoenberg and Muir calculus, Chapter I presented a method to obtain the elastic properties of the unfractured background by separating the effects of fractures from a fractured medium. Thus it becomes possible to analyze fracture effects separately, without interference from the background anisotropy.

Nichols et al. [1989] modified the Schoenberg and Muir calculus by introducing compliances rather than stiffnesses. This substitution greatly simplifies the forward calculations of elastic moduli for composite media.

Revisiting the Schoenberg and Muir Calculus

Hooke's law for a general linear elastic medium, in condensed notation [Auld, 1973], is

$$\epsilon = \mathbf{S}\sigma, \quad (35)$$

where the stress and strain tensor components in condensed and normal notation, respectively, are

$$\begin{aligned} [\sigma_1, \sigma_2, \sigma_3, \sigma_4, \sigma_5, \sigma_6]^t &\equiv [\sigma_{11}, \sigma_{22}, \sigma_{33}, \sigma_{23}, \sigma_{13}, \sigma_{12}]^t, \\ [\epsilon_1, \epsilon_2, \epsilon_3, \epsilon_4, \epsilon_5, \epsilon_6]^t &\equiv [\epsilon_{11}, \epsilon_{22}, \epsilon_{33}, 2\epsilon_{23}, 2\epsilon_{13}, 2\epsilon_{12}]^t, \end{aligned} \quad (36)$$

and \mathbf{S} is the symmetric 6×6 compliance matrix (the inverse of the stiffness matrix \mathbf{C}). Superscript t denotes the transpose.

In a layered medium with the x_3 axis normal to the layers (Fig. 2.1), tractions on the planes parallel to layering, i.e. $\sigma_3, \sigma_4, \sigma_5$, and deformations in the planes of the layering, i.e., $\epsilon_1, \epsilon_2, \epsilon_6$, are assumed constant through the stack of layers. Tractions

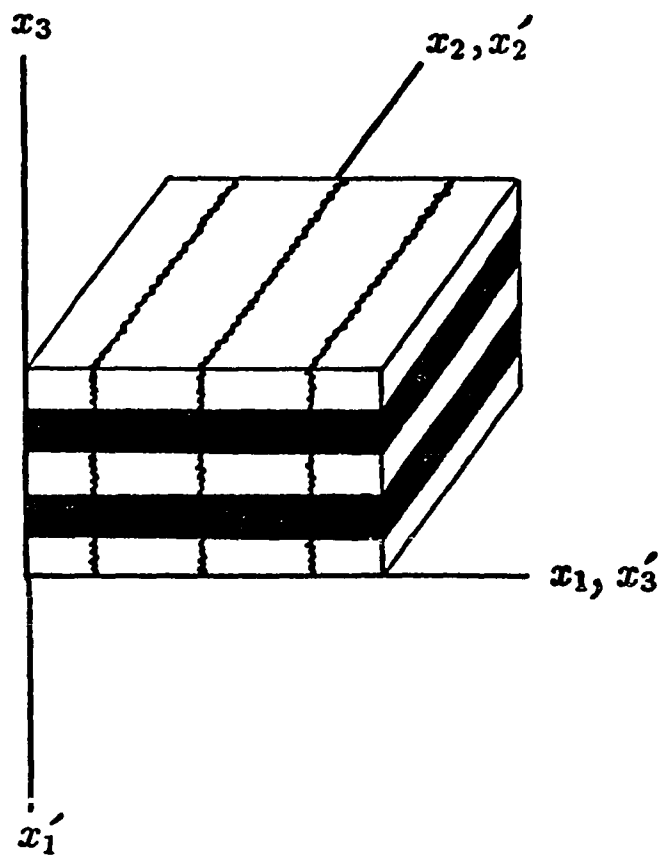


Figure 2.1 Vertical fractures in a layered medium.

in the planes of the layering, i.e., $\sigma_1, \sigma_2, \sigma_6$, and deformations on the planes parallel to the layering, i.e., $\epsilon_3, \epsilon_4, \epsilon_5$, vary from layer to layer.

Therefore it is convenient to subdivide \mathbf{S} into the four parts relating stress and strain Normal and Tangential to the layering (indexed by N and T). Normal ϵ_{ij} and σ_{ij} are those with either i or j equal to 3, or in condensed notation, ϵ_i, σ_i with $i = 3, 4, 5$. Tangential components (ϵ_{ij} and σ_{ij}) have all $i, j \neq 3$ or in condensed notation, ϵ_i, σ_i with $i = 1, 2, 6$.

The strain-stress relation, equation (35), can then be rewritten

$$\begin{bmatrix} \epsilon_T \\ \epsilon_N \end{bmatrix} = \begin{bmatrix} \mathbf{S}_{TT} & \mathbf{S}_{TN} \\ \mathbf{S}_{TN}^t & \mathbf{S}_{NN} \end{bmatrix} \begin{bmatrix} \sigma_T \\ \sigma_N \end{bmatrix} \quad (37)$$

with

$$\epsilon_T = [\epsilon_1, \epsilon_2, \epsilon_6]^t, \quad \epsilon_N = [\epsilon_3, \epsilon_4, \epsilon_5]^t, \quad \sigma_T = [\sigma_1, \sigma_2, \sigma_6]^t, \quad \sigma_N = [\sigma_3, \sigma_4, \sigma_5]^t,$$

$$\mathbf{S}_{NN} = \begin{bmatrix} s_{33} & s_{34} & s_{35} \\ s_{34} & s_{44} & s_{45} \\ s_{35} & s_{45} & s_{55} \end{bmatrix}, \quad \mathbf{S}_{TN} = \begin{bmatrix} s_{13} & s_{14} & s_{15} \\ s_{23} & s_{24} & s_{25} \\ s_{36} & s_{46} & s_{56} \end{bmatrix}, \quad \mathbf{S}_{TT} = \begin{bmatrix} s_{11} & s_{12} & s_{16} \\ s_{12} & s_{22} & s_{26} \\ s_{16} & s_{26} & s_{66} \end{bmatrix},$$

where the s_{ij} are the symmetric elements of \mathbf{S} . Note that the compliance matrix in this system, equation (37), is also symmetric. It is important to realize, however, that this notation is general and holds for any orientation of the coordinate system with respect to the layering.

Nichols et al. [1989] followed the Schoenberg and Muir procedure using Backus' averaging techniques [1962] to determine the long wavelength equivalent compliances for layered media. We, therefore, follow essentially that procedure.

A depth section of thickness H is composed of layers (in welded contact) with different densities and elastic moduli. Several of the interleaved layers (in H) may have the same properties (indexed by i). The averaging technique lumps all layers of identical properties (in H) together, making up a total thickness H_i , with property i , so that $H = \sum_i H_i$. The geometrical and physical model parameters of the i th constituent in H for the long wavelength approximation are $H_i, (\rho, \mathbf{S}_{NN}, \mathbf{S}_{TN}, \mathbf{S}_{TT})_i$.

The physical properties transform to the group element of \mathbf{G}_i by

$$\begin{bmatrix} \rho \\ \mathbf{S}_{NN} \\ \mathbf{S}_{TN} \\ \mathbf{S}_{TT} \end{bmatrix}_i \rightarrow \begin{bmatrix} \mathbf{S}_{NN} & -\mathbf{S}_{TN}^t \mathbf{S}_{TT}^{-1} \mathbf{S}_{TN} \\ & -\mathbf{S}_{TT}^{-1} \mathbf{S}_{TN} \\ & & \mathbf{S}_{TT}^{-1} \end{bmatrix}_i \equiv \begin{bmatrix} g(2) \\ \mathbf{g}(3) \\ \mathbf{g}(4) \\ \mathbf{g}(5) \end{bmatrix}_i = \mathbf{G}_i. \quad (38)$$

For any \mathbf{G}_i where $\mathbf{g}(5)_i^{-1}$ exists, the physical model parameters are returned by:

$$\mathbf{G}_i \rightarrow \begin{bmatrix} g(2) \\ \mathbf{g}(3) & +\mathbf{g}(4)^t \mathbf{g}(5)^{-1} \mathbf{g}(4) \\ & -\mathbf{g}(5)^{-1} \mathbf{g}(4) \\ & & \mathbf{g}(5)^{-1} \end{bmatrix}_i \equiv \begin{bmatrix} \rho \\ \mathbf{S}_{NN} \\ \mathbf{S}_{TN} \\ \mathbf{S}_{TT} \end{bmatrix}_i. \quad (39)$$

To avoid confusion, the original Schoenberg and Muir indexing for elements in \mathbf{G} is conserved. The long wavelength physical properties of the total section H are therefore described by the group elements $\overline{\mathbf{G}}$ where

$$H\overline{\mathbf{G}} = \sum_i H_i \mathbf{G}_i \quad \text{or} \quad \overline{\mathbf{G}} = \sum_i \frac{H_i}{H} \mathbf{G}_i. \quad (40)$$

This gives, for example, the average density

$$\overline{\rho} = \overline{g(2)} = \sum_i \frac{H_i}{H} \rho_i \quad (41)$$

and

$$\overline{g(5)} = \sum_i \frac{H_i}{H} \mathbf{S}_{TT_i}^{-1} = \overline{\mathbf{S}_{TT}^{-1}}, \quad (42)$$

gives

$$\overline{\mathbf{S}_{TT}} = \left[\sum_i \frac{H_i}{H} \mathbf{S}_{TT_i}^{-1} \right]^{-1}.$$

This is essentially the same group element formulation presented by Schoenberg and Muir [1989] except that the elements are defined in terms of compliances rather than stiffnesses, and the geometrical parameters, H and H_i , have been separated from the physical properties expressed in \mathbf{G} and \mathbf{S} .

The Fracture Model

The strain-stress relation of any fracture set embedded in an elastic medium can be characterized by a symmetric, non-negative definite 3×3 matrix [Schoenberg and Douma, 1988], requiring only six parameters to completely describe the most general elastic response due to the fractures. These parameters are the components of the fracture compliance matrix

$$\mathbf{Z} = \begin{bmatrix} Z_{11} & Z_{12} & Z_{13} \\ Z_{12} & Z_{22} & Z_{23} \\ Z_{13} & Z_{23} & Z_{33} \end{bmatrix}. \quad (43)$$

The elements of \mathbf{Z} correspond to the slip of the fractures in a unit thickness as a linear function of all the traction components acting normal to the fractures. Therefore, while the traction across a surface is continuous, the displacement can be discontinuous to first order. Call the \mathbf{G} -element corresponding to such a fracture set \mathbf{G}_f . The components of \mathbf{G}_f were first given explicitly by [Schoenberg and Muir, 1989] and for our modified formulation are

$$g_f(2) = 0, \quad g_f(3) = \mathbf{Z}, \quad g_f(4) = 0, \quad g_f(5) = 0. \quad (44)$$

With the exception of $g_f(3)$, the components of \mathbf{G}_f are all zero. Therefore, $g(3)_i$ of a \mathbf{G}_i is the only element that changes as a result of fracturing. Since $g_f(4)$ and $g_f(5)$ are zero, fracturing only affects \mathbf{S}_{NN_i} , but does not affect \mathbf{S}_{TN_i} or \mathbf{S}_{TT_i} . Consequently, as equation (37) shows, only the elastic response ϵ_N to σ_N is modified in a fracture oriented coordinate system. Therefore, as long as a primed (fracture oriented) coordinate system is chosen so that the normal to the fracture planes is aligned with the normal (the x'_3 axis) defining these submatrices (now \mathbf{S}'_{NN} , \mathbf{S}'_{TN} , and \mathbf{S}'_{TT}), fracturing rock is as simple as adding the fracture system \mathbf{F}' to \mathbf{S}'_b , the rotated background system \mathbf{S}_b . This process yields the same results as the revised Schoenberg and Muir transformations derived by Nichols et al. [1989] but with fewer calculations.

For a set of fractures in which the x'_3 axis is perpendicular to the fracture planes,

Nichols et al. [1989] showed that the change in the compliance matrix is

$$\Delta \mathbf{S}' = \mathbf{F}' = \begin{bmatrix} 0 & 0 & 0 & 0 & 0 & 0 \\ 0 & 0 & 0 & 0 & 0 & 0 \\ 0 & 0 & Z_{11} & Z_{12} & Z_{13} & 0 \\ 0 & 0 & Z_{12} & Z_{22} & Z_{23} & 0 \\ 0 & 0 & Z_{13} & Z_{23} & Z_{33} & 0 \\ 0 & 0 & 0 & 0 & 0 & 0 \end{bmatrix} = \mathbf{E}' \mathbf{Z} \mathbf{E} \quad (45)$$

with

$$\mathbf{E} = \begin{bmatrix} 0 & 0 & 1 & 0 & 0 & 0 \\ 0 & 0 & 0 & 1 & 0 & 0 \\ 0 & 0 & 0 & 0 & 1 & 0 \end{bmatrix}. \quad (46)$$

The following calculations show that eigencoordinates and compliances of different fracture sets can be transformed individually to those of the background compliances \mathbf{S}_b . Therefore any number of sets can be included, provided there is no nonlinear interaction between constituent fracture systems.

A coordinate change for a compliance matrix \mathbf{S}' is obtained by the Bond transformation [Auld, 1973], so that

$$\mathbf{N} \mathbf{S}' \mathbf{N}^t = \mathbf{S} \quad (47)$$

where

$$\mathbf{N} = \begin{bmatrix} a_{xx}^2 & a_{xy}^2 & a_{xz}^2 & a_{xy}a_{xz} & a_{xz}a_{xx} & a_{xx}a_{xy} \\ a_{yx}^2 & a_{yy}^2 & a_{yz}^2 & a_{yy}a_{yz} & a_{yz}a_{yx} & a_{yx}a_{yy} \\ a_{zx}^2 & a_{zy}^2 & a_{zz}^2 & a_{zy}a_{zz} & a_{zz}a_{zx} & a_{zx}a_{zy} \\ 2a_{yx}a_{zx} & 2a_{yy}a_{zy} & 2a_{yz}a_{zz} & a_{yy}a_{zz} + a_{yz}a_{zy} & a_{yx}a_{zz} + a_{yz}a_{zx} & a_{yy}a_{zx} + a_{yx}a_{zy} \\ 2a_{zx}a_{xx} & 2a_{zy}a_{xy} & 2a_{zz}a_{xz} & a_{xy}a_{zz} + a_{xz}a_{zy} & a_{xz}a_{zx} + a_{xx}a_{zz} & a_{xx}a_{zy} + a_{xy}a_{zx} \\ 2a_{xx}a_{yx} & 2a_{xy}a_{yy} & 2a_{xz}a_{yz} & a_{xy}a_{yz} + a_{xz}a_{yy} & a_{xz}a_{yx} + a_{xx}a_{yz} & a_{xx}a_{yy} + a_{xy}a_{yx} \end{bmatrix}. \quad (48)$$

The a_{ij} are the direction cosines of the 'new' coordinate axes, (x_1, x_2, x_3) , with respect to the 'old' coordinate axes, (x'_1, x'_2, x'_3) in which the fracture compliance matrix \mathbf{F}' , equation (45), is defined.

The fracture compliance matrix \mathbf{Z} in \mathbf{F}' contributes only to the \mathbf{S}'_{NN} portion of \mathbf{S}' that appears linearly in the $g(3)$ element of equations (38) or (39). Therefore, (in x'_1, x'_2, x'_3) the long wavelength equivalent \mathbf{S}' of a fractured transversely isotropic

medium is then simply the sum of the fracture matrix \mathbf{F}' and the transformed background compliance matrix, $\mathbf{S}'_b = \mathbf{N}^{-1}\mathbf{S}_b(\mathbf{N}^t)^{-1}$,

$$\mathbf{S}' = \mathbf{N}^{-1}\mathbf{S}_b(\mathbf{N}^t)^{-1} + \mathbf{F}' . \quad (49)$$

Transforming \mathbf{S}' back from fracture eigencoordinates (x'_1, x'_2, x'_3) to (x_1, x_2, x_3) then yields

$$\mathbf{S} = \mathbf{N}\mathbf{S}'\mathbf{N}^t = \mathbf{S}_b + \mathbf{N}\mathbf{F}'\mathbf{N}^t = \mathbf{S}_b + \mathbf{F} \equiv \mathbf{S}_b + \Delta\mathbf{S} . \quad (50)$$

The fracture contribution $\Delta\mathbf{S}$ to the compliance \mathbf{S} appears as being rotated from its eigencoordinates into those of our observations. Different fracture sets have different physical properties, \mathbf{F}'_i , and eigencoordinates (expressed by the \mathbf{N}_i). As long as there are no nonlinear interactions, the compliance matrices for the background medium and the rotated fracture \mathbf{F}' add together so that for n fracture sets

$$\mathbf{S} = \mathbf{S}_b + \sum_{i=1}^n \Delta\mathbf{S}_i . \quad (51)$$

Example Involving Vertical Fractures

A horizontally layered medium (transversely isotropic) embedded with vertical fractures has orthorhombic symmetry (see Chapter I). In the observation coordinates of Fig. 2.1, the compliance matrix is therefore

$$\mathbf{S}_b + \Delta\mathbf{S} = \mathbf{S} = \begin{bmatrix} s_{11} & s_{12} & s_{13} & 0 & 0 & 0 \\ s_{12} & s_{22} & s_{23} & 0 & 0 & 0 \\ s_{13} & s_{23} & s_{33} & 0 & 0 & 0 \\ 0 & 0 & 0 & s_{44} & 0 & 0 \\ 0 & 0 & 0 & 0 & s_{55} & 0 \\ 0 & 0 & 0 & 0 & 0 & s_{66} \end{bmatrix} \quad (52)$$

and the fracture contribution, $\Delta\mathbf{S}$, can be separated from the background contribution, \mathbf{S}_b .

Vertical fractures with at most orthorhombic symmetry can be represented in their eigencoordinates as

$$\mathbf{Z} = \begin{bmatrix} Z_N & 0 & 0 \\ 0 & Z_2 & 0 \\ 0 & 0 & Z_3 \end{bmatrix} \quad (53)$$

and, consequently,

$$\Delta \mathbf{S} = \mathbf{N} \mathbf{F}' \mathbf{N}' = \mathbf{N} \mathbf{E}' \mathbf{Z} \mathbf{E}' \mathbf{N}'^t, \quad (54)$$

where \mathbf{E} is given in equation (46). The horizontal x_2 axis is chosen along the surface strike of the fracture plane and is identical to x'_2 . Choosing the eigen axis x'_3 normal to the fracture planes (horizontal with $x'_3 = x_1$), the transformation of \mathbf{F}' from the $(x'_1 = -x_3, x'_2 = x_2, x'_3 = x_1)$ into the (x_1, x_2, x_3) system requires a $\phi = -\pi/2$ rotation about the x_2 axis (Fig. 2.1). Equation (48) gives

$$\mathbf{N} = \begin{bmatrix} 0 & 0 & 1 & 0 & 0 & 0 \\ 0 & 1 & 0 & 0 & 0 & 0 \\ 1 & 0 & 0 & 0 & 0 & 0 \\ 0 & 0 & 0 & 0 & 0 & -1 \\ 0 & 0 & 0 & 0 & -1 & 0 \\ 0 & 0 & 0 & 1 & 0 & 0 \end{bmatrix}. \quad (55)$$

Therefore,

$$\Delta \mathbf{S} = \mathbf{N} \mathbf{F}' \mathbf{N}' = \begin{bmatrix} Z_N & 0 & 0 & 0 & 0 & 0 \\ 0 & 0 & 0 & 0 & 0 & 0 \\ 0 & 0 & 0 & 0 & 0 & 0 \\ 0 & 0 & 0 & 0 & 0 & 0 \\ 0 & 0 & 0 & 0 & Z_3 & 0 \\ 0 & 0 & 0 & 0 & 0 & Z_2 \end{bmatrix}. \quad (56)$$

The long wavelength equivalent medium of a transversely isotropic background embedded with a set of vertical fractures is $\mathbf{S} = \mathbf{S}_b + \Delta \mathbf{S}$, equation (49). Removing a set of vertical fractures is accomplished by $\mathbf{S}_b = \mathbf{S} - \Delta \mathbf{S}$:

$$\mathbf{S}_b = \begin{bmatrix} s_{11_b} & s_{12_b} & s_{13_b} & 0 & 0 & 0 \\ s_{12_b} & s_{22_b} & s_{23_b} & 0 & 0 & 0 \\ s_{13_b} & s_{23_b} & s_{33_b} & 0 & 0 & 0 \\ 0 & 0 & 0 & s_{44_b} & 0 & 0 \\ 0 & 0 & 0 & 0 & s_{55_b} & 0 \\ 0 & 0 & 0 & 0 & 0 & s_{66_b} \end{bmatrix} = \begin{bmatrix} s_{11} - Z_N & s_{12} & s_{13} & 0 & 0 & 0 \\ s_{12} & s_{22} & s_{23} & 0 & 0 & 0 \\ s_{13} & s_{23} & s_{33} & 0 & 0 & 0 \\ 0 & 0 & 0 & s_{44} & 0 & 0 \\ 0 & 0 & 0 & 0 & s_{55} - Z_3 & 0 \\ 0 & 0 & 0 & 0 & 0 & s_{66} - Z_2 \end{bmatrix}, \quad (57)$$

where the s_{ij} can be determined from seismic velocity measurements following the section of Chapter I entitled Measurements Sufficient to Determine Orthorhombic Moduli, page 15.

The unknown fracture compliances, Z_i , can be determined by satisfying the four conditions required for the background medium to be transversely isotropic,

$$s_{44_b} = s_{55_b}, \quad s_{13_b} = s_{23_b}, \quad s_{11_b} = s_{22_b}, \quad s_{12_b} = s_{11_b} - \frac{1}{2}s_{66_b}. \quad (58)$$

Equation (57) then gives for $s_{44_b} = s_{55_b}$ and $s_{11_b} = s_{22_b}$, respectively,

$$Z_3 = s_{55} - s_{44}, \quad (59)$$

$$Z_N = s_{11} - s_{22}, \quad (60)$$

and for $s_{12_b} = s_{11_b} - \frac{1}{2}s_{66_b}$, using the result for Z_N of equation (60),

$$Z_2 = 2(s_{11} - s_{22}) + s_{66}. \quad (61)$$

The condition $s_{13_b} = s_{23_b}$ reveals that, rather than the usual nine parameters required to define general orthorhombic media, only eight independent parameters are necessary to define a vertically fractured, horizontally stratified medium. This reduction enables a simpler experimental design to recover the s_{ij} from independent wave velocity measurements. However, if nine independent measurements are available, then the condition $s_{13_b} = s_{23_b}$ provides a test for determining whether and how close the subject medium conforms to the model.

The compliance matrix, \mathbf{S} , is the inverse of the stiffness matrix, \mathbf{C} . The fracture effects were isolated in Chapter I but were defined in terms of measured stiffness moduli. To verify these results, the measured compliances of equation (52) must be defined as functions of c_{ij} . The stiffness matrix of an orthorhombic medium is

$$\mathbf{C} = \begin{bmatrix} c_{11} & c_{12} & c_{13} & 0 & 0 & 0 \\ c_{12} & c_{22} & c_{23} & 0 & 0 & 0 \\ c_{13} & c_{23} & c_{33} & 0 & 0 & 0 \\ 0 & 0 & 0 & c_{44} & 0 & 0 \\ 0 & 0 & 0 & 0 & c_{55} & 0 \\ 0 & 0 & 0 & 0 & 0 & c_{66} \end{bmatrix}. \quad (62)$$

The inverse of this matrix gives the elements of \mathbf{S} of equation (52) as functions of c_{ij} :

$$s_{11} = \frac{c_{23}^2 - c_{22}c_{33}}{X}, \quad s_{12} = \frac{c_{12}c_{33} - c_{13}c_{23}}{X}, \quad s_{13} = \frac{c_{13}c_{22} - c_{12}c_{23}}{X},$$

$$s_{22} = \frac{c_{13}^2 - c_{11}c_{33}}{X}, \quad s_{23} = \frac{c_{11}c_{23} - c_{12}c_{13}}{X}, \quad s_{33} = \frac{c_{12}^2 - c_{11}c_{22}}{X},$$

$$s_{44} = \frac{1}{c_{44}}, \quad s_{55} = \frac{1}{c_{55}}, \quad s_{66} = \frac{1}{c_{66}}, \quad (63)$$

where X is the determinant of the 3×3 submatrix of \mathbf{C} :

$$X = c_{13}^2 c_{22} - 2c_{12}c_{13}c_{23} + c_{11}c_{23}^2 + c_{12}^2 c_{33} - c_{11}c_{22}c_{33}. \quad (64)$$

Substituting the s_{ij} of equation (63) into equations (59), (60), and (61) we obtain

$$Z_3 = \frac{1}{c_{55}} - \frac{1}{c_{44}}, \quad (65)$$

$$Z_N = \frac{c_{23} - c_{13}}{c_{11}c_{23} - c_{12}c_{13}}, \quad (66)$$

and

$$Z_2 = \frac{1}{c_{66}} - \frac{2c_{13}}{c_{11}c_{23} - c_{12}c_{13}}. \quad (67)$$

The condition $s_{13_b} = s_{23_b}$ of equation (58), with the relations of equation (63), gives

$$c_{22} = \frac{c_{23}}{c_{13}}(c_{11} + c_{12}) - c_{12}. \quad (68)$$

Results (65)-(68) are identical to those determined in Chapter I, equations (25), (27), (29), and (13), but with fewer calculations by avoiding altogether the Schoenberg and Muir transformations.

Discussion

Fracture-induced anisotropy is more easily understood when defined in terms of compliances rather than stiffnesses. In particular, isolation of the effects of a single fracture set, as demonstrated in Chapter I, becomes both mathematically simple and computationally concise. Although not specifically demonstrated here, it is clear that this treatment generalizes to multiple fracture sets.

CHAPTER III

SEPARATING CONSTITUENTS IN COMPLEX ANISOTROPIC MEDIA

Background

This chapter presents a separation technique applicable to general fracture systems. We assume that the global elastic moduli have been ‘measured’ by some method. The technique can then be applied to separate out the contributions of the fractures and the background, and to determine the fracture dip angle. The method reveals several new relationships among the measured elastic constants which constrain the complexity of the constituents’ symmetry.

Once elastic compliance moduli for a region are estimated from seismic velocity measurements, the unknown fracture dip angle, and the unknown fracture and background compliances can be determined separately following the method presented in Chapter II by imposing the symmetry conditions of the background, all of which constrain the global elastic constants of the compound medium.

The number of symmetry constraints increases as the background becomes more symmetric. Additional constraints (from higher symmetry backgrounds) reduce the effective number of elastic compliance constants. These constraints provide tests for evaluating whether and how well the real medium conforms to the model.

Modeling a Fractured Medium

Building on the Schoenberg and Douma results [1988], Nichols et al. [1989] showed that, for any background medium, a set of horizontal fractures will change the compliance matrix of the background by

$$\mathbf{F}' = \mathbf{E}'\mathbf{Z}\mathbf{E} = \begin{bmatrix} 0 & 0 & 0 & 0 & 0 & 0 \\ 0 & 0 & 0 & 0 & 0 & 0 \\ 0 & 0 & Z_N & Z_{NH} & Z_{NV} & 0 \\ 0 & 0 & Z_{NH} & Z_H & Z_{HV} & 0 \\ 0 & 0 & Z_{NV} & Z_{HV} & Z_V & 0 \\ 0 & 0 & 0 & 0 & 0 & 0 \end{bmatrix} \quad (69)$$

with

$$\mathbf{E} = \begin{bmatrix} 0 & 0 & 1 & 0 & 0 & 0 \\ 0 & 0 & 0 & 1 & 0 & 0 \\ 0 & 0 & 0 & 0 & 1 & 0 \end{bmatrix}. \quad (70)$$

The subscripts N , H , and V correspond to compliance components in the normal, horizontal, and vertical directions, respectively, relative to the fracture planes.

The goal of this chapter is to find the physical properties of the fractures and of the background material (expressed in \mathbf{S}_b) by removing the fracture contributions (\mathbf{F}) from the overall compliance matrix \mathbf{S} , in equation (35). Consider a set of parallel fractures in which ϕ is the fracture dip angle (Fig. 3.1). This geometry gives rise to monoclinic symmetry. In plan view, the plane of symmetry is vertical, normal to the fracture strike. Since only elastic SH waves decouple in the single symmetry plane, the direction in which this occurs fixes the observation coordinates (x_1, x_2, x_3) . We choose x_1 as horizontal normal to the fracture strike, x_2 horizontal along strike, and x_3 vertical upward. We must now determine the compliance contribution of the fracture system, \mathbf{F} , relative to the observation coordinates in which \mathbf{S} has been 'measured'. The starting point is the fracture compliance \mathbf{F}' in the eigencoordinates of the fracture system (x'_1, x'_2, x'_3) .

In the fracture eigencoordinates (the primed system), the global compliance matrix \mathbf{S}' is given by

$$\mathbf{S}' = \mathbf{S}'_b + \mathbf{F}'; \quad (71)$$

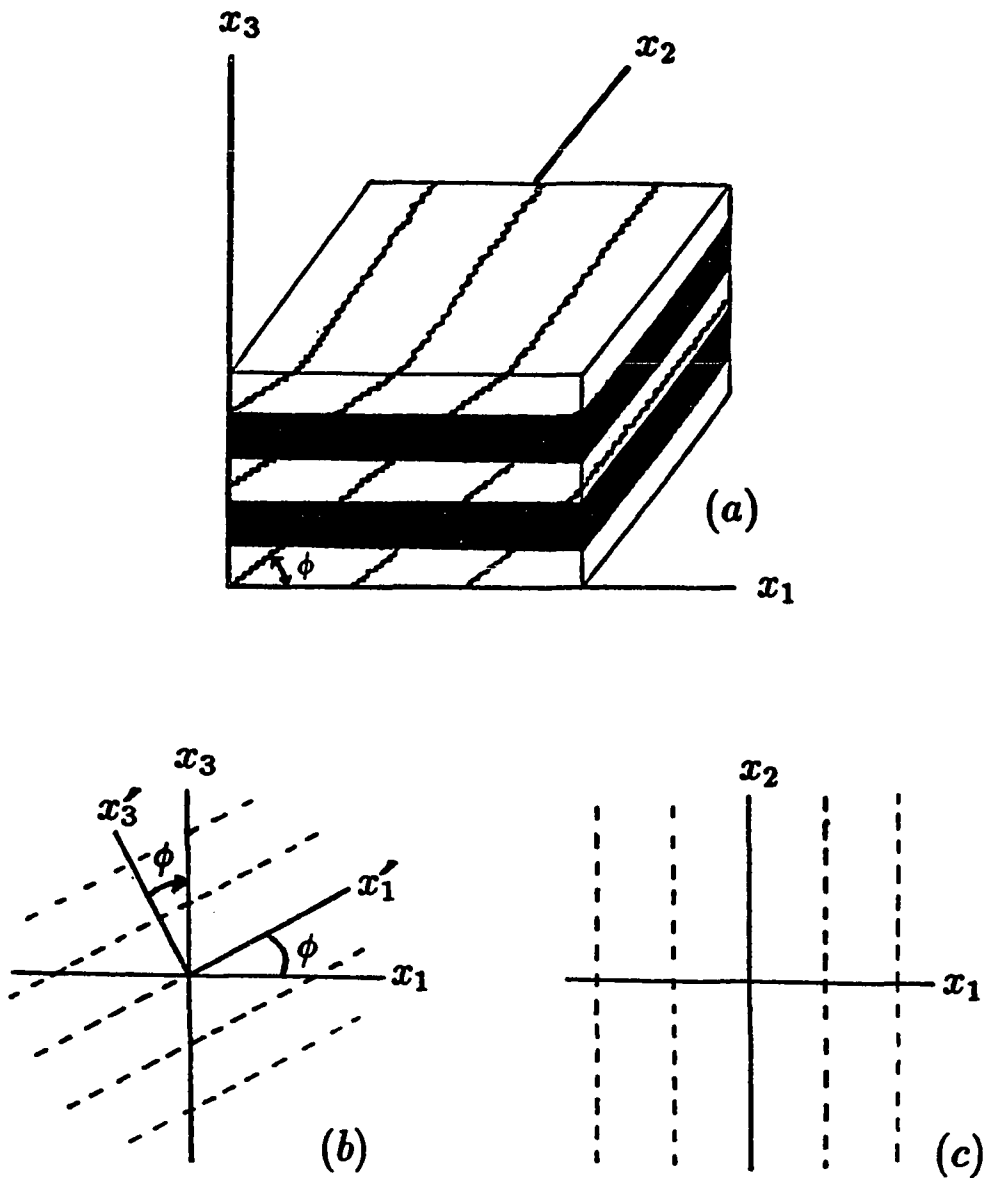


Figure 3.1: Geometry of the Monoclinic System:

- (a) General 3D fractured, layered medium.
- (b) The vertical x_1 - x_3 plane shows ϕ as the fracture dip angle.
- (c) Plan-view shows the fracture strike parallels the x_2 axis.

simple addition of the unfractured background and fracture compliances, where \mathbf{F}' is given by equation (69) and \mathbf{S}'_b is the compliance matrix of the unfractured background material (in primed coordinates). A coordinate change of a compliance matrix (from \mathbf{S}' back to \mathbf{S}) is obtained by the Bond transformation matrix \mathbf{N} [Auld, 1973, p.75] so that

$$\mathbf{S} = \mathbf{N}\mathbf{S}'\mathbf{N}^t = \mathbf{N}(\mathbf{S}'_b + \mathbf{F}')\mathbf{N}^t = \mathbf{S}_b + \mathbf{N}\mathbf{F}'\mathbf{N}^t = \mathbf{S}_b + \mathbf{F}. \quad (72)$$

Fig. 3.1 shows that the coordinate transformation from $(x'_1, x'_2 = x_2, x'_3)$ to (x_1, x_2, x_3) is a simple rotation about the x_2 axis by the angle ϕ :

$$\mathbf{x} = \mathbf{A}\mathbf{x}' \quad (73)$$

with

$$\mathbf{A} = \begin{bmatrix} c & 0 & s \\ 0 & 1 & 0 \\ -s & 0 & c \end{bmatrix}, \quad (74)$$

where

$$c = \cos \phi, \quad s = \sin \phi.$$

The elements of \mathbf{A} are the direction cosines required for the 6×6 Bond transformation \mathbf{N} of equation (48).

As equation (72) shows, fracturing rock is as simple as adding the contribution of the fractures relative to observation coordinates, \mathbf{F} , to the background rock, \mathbf{S}_b . By expanding $\mathbf{N}\mathbf{F}'\mathbf{N}^t = \mathbf{F}$ we obtain

$$\mathbf{F} = \begin{bmatrix} F_{11} & 0 & F_{13} & F_{14} & F_{15} & F_{16} \\ 0 & 0 & 0 & 0 & 0 & 0 \\ F_{13} & 0 & F_{33} & F_{34} & F_{35} & F_{36} \\ F_{14} & 0 & F_{34} & F_{44} & F_{45} & F_{46} \\ F_{15} & 0 & F_{35} & F_{45} & F_{55} & F_{56} \\ F_{16} & 0 & F_{36} & F_{46} & F_{56} & F_{66} \end{bmatrix}. \quad (75)$$

The elements of \mathbf{F} are

$$\begin{aligned}
F_{11} &= s^2 c^2 Z_V + s^4 Z_N + 2cs^3 Z_{NV}, \\
F_{13} &= -c^2 s^2 Z_V + c^2 s^2 Z_N + cs(c^2 - s^2) Z_{NV}, \\
F_{33} &= c^2 s^2 Z_V + c^4 Z_N - 2c^3 s Z_{NV}, \\
F_{15} &= cs(c^2 - s^2) Z_V + 2cs^3 Z_N + s^2(3c^2 - s^2) Z_{NV}, \\
F_{35} &= -cs(c^2 - s^2) Z_V + 2c^3 s Z_N + c^2(c^2 - 3s^2) Z_{NV}, \\
F_{55} &= (c^2 - s^2)^2 Z_V + 4c^2 s^2 Z_N + 4cs(c^2 - s^2) Z_{NV}, \\
F_{44} &= c^2 Z_H, \quad F_{46} = cs Z_H, \quad F_{66} = s^2 Z_H, \\
F_{14} &= cs^2 Z_{NH} + c^2 s Z_{HV}, \quad F_{16} = s^3 Z_{NH} + cs^2 Z_{HV}, \\
F_{34} &= c^3 Z_{NH} - c^2 s Z_{HV}, \quad F_{36} = c^2 s Z_{NH} - cs^2 Z_{HV}, \\
F_{45} &= 2c^2 s Z_{NH} + c(c^2 - s^2) Z_{HV}, \quad F_{56} = 2cs^2 Z_{NH} + s(c^2 - s^2) Z_{HV}.
\end{aligned} \tag{76}$$

The matrix \mathbf{F} in equation (75) represents the change of compliance resulting from the presence of a single fracture set. Its form indicates that even an isotropic background containing a set of general fractures (where at least five of the six elements of \mathbf{Z} are nonzero) has triclinic symmetry.

This chapter addresses media with at most monoclinic symmetry, since lower symmetries are too complicated to be of much geological interest. To obtain monoclinic symmetry, the fracture slip along strike must be uncoupled from the normal slip and from the tangential slip in the x_1 direction, i.e., $Z_{HN} \equiv 0$ and $Z_{VH} \equiv 0$, respectively. When $Z_{VH} = Z_{HN} \equiv 0$ in (75) then $F_{i4} = F_{4j} \equiv 0$ for all i, j , so that \mathbf{F} will generate an equivalent medium that is monoclinic with the x_1, x_3 plane as the plane of mirror symmetry. The s_{12} , s_{22} , and s_{23} compliances are not affected when the fracture strike is the x_2 axis. Since $s_{25} = 0$, the number of parameters in \mathbf{S} is reduced from thirteen to twelve.

Any number of fracture sets can be included in a medium. Once each fracture system is aligned with the coordinates of the background compliance matrix, \mathbf{F} need

only be added to \mathbf{S}_b to find the equivalent properties of the fractured medium, \mathbf{S} . Since the change in compliance is independent of the background properties, adding and removing fractures is commutative as long as there is no nonlinear interaction between the fracture sets. The compliance matrix for n fracture sets is

$$\mathbf{S} = \mathbf{S}_b + \sum_i^n \mathbf{N}_i \mathbf{F}_i' \mathbf{N}_i^t = \mathbf{S}_b + \sum_{i=1}^n \mathbf{F}_i. \quad (77)$$

When a fractured medium has hexagonal symmetry, it has only two independent fracture parameters. These parameters are the normal compliance, Z_N , and the tangential compliance, $Z_T (= Z_V \equiv Z_H)$. In a fracture system with hexagonal symmetry, the tangential fracture displacement is colinear with the tangential component of the traction and the normal and tangential responses are uncoupled. Note that if $Z_T \geq \frac{4}{3}Z_N \geq 0$, then fractured isotropic media can be simulated by isotropic layering [Schoenberg and Douma, 1988].

Three parameters, Z_N , Z_H , and Z_V , define an orthorhombic fracture system. The tangential fracture displacement and the tangential component of the traction are not colinear, so $Z_V \neq Z_H$. The normal compliance, Z_N , however, is uncoupled from the tangential compliances and each of its elements, Z_{NH} , Z_{NV} , and Z_{HV} , is zero. A monoclinic fracture system requires four independent parameters. Although $Z_{NH} = Z_{HV} \equiv 0$, the slip in the x_1 direction could be uncoupled from the normal slip, i.e., $Z_{NV} \neq 0$. For practical purposes, however, it is assumed that $Z_{NV} \equiv 0$. Therefore the fracture system for this model has at most orthorhombic symmetry.

A Procedure for Extracting Fracture Compliances from Measured Moduli

After the compliance moduli are measured, this separation method reveals the three fracture compliances, the fracture dip angle, and the elastic moduli of the unfractured background.

Compliance measurements from a fractured transversely isotropic medium has a strain-stress matrix with this monoclinic symmetry:

$$\mathbf{S} = \begin{bmatrix} s_{11} & s_{12} & s_{13} & 0 & s_{15} & 0 \\ s_{12} & s_{22} & s_{23} & 0 & 0 & 0 \\ s_{13} & s_{23} & s_{33} & 0 & s_{35} & 0 \\ 0 & 0 & 0 & s_{44} & 0 & s_{46} \\ s_{15} & 0 & s_{35} & 0 & s_{55} & 0 \\ 0 & 0 & 0 & s_{46} & 0 & s_{66} \end{bmatrix}. \quad (78)$$

We wish to find the fracture matrix \mathbf{Z} , the fracture dip angle ϕ , and the background compliance matrix. So the result is

$$\mathbf{S}_b = \mathbf{S} - \mathbf{F}. \quad (79)$$

Therefore, for

$$\mathbf{Z} = \begin{bmatrix} Z_N & 0 & 0 \\ 0 & Z_H & 0 \\ 0 & 0 & Z_V \end{bmatrix}, \quad (80)$$

the elements of \mathbf{S}_b in the observation coordinates are

$$\begin{aligned} s_{12_b} &= s_{12}, & s_{22_b} &= s_{22}, & s_{23_b} &= s_{23}, \\ s_{11_b} &= s_{11} - c^2 s^2 Z_V - s^4 Z_N, & s_{13_b} &= s_{13} + c^2 s^2 Z_V - c^2 s^2 Z_N, \\ s_{33_b} &= s_{33} - c^2 s^2 Z_V - c^4 Z_N, & s_{15_b} &= s_{15} - cs(c^2 - s^2)Z_V - 2cs^3 Z_N, \\ s_{35_b} &= s_{35} + cs(c^2 - s^2)Z_V - 2c^3 s Z_N, & s_{55_b} &= s_{55} - (c^2 - s^2)^2 Z_V - 4c^2 s^2 Z_N, \\ s_{44_b} &= s_{44} - c^2 Z_H, & s_{46_b} &= s_{46} - cs Z_H, & s_{66_b} &= s_{66} - s^2 Z_H. \end{aligned} \quad (81)$$

If the background is transversely isotropic, the three unknown fracture compliances and angle ϕ can be determined by imposing the background symmetry conditions:

$$\begin{aligned} s_{44_b} &= s_{55_b}, & s_{13_b} &= s_{23_b}, & s_{11_b} &= s_{22_b}, & s_{12_b} &= s_{11_b} - \frac{1}{2}s_{66_b}, \\ s_{15_b} &= s_{35_b} = s_{46_b} & \equiv 0. \end{aligned} \quad (82)$$

With the geometric constraint $c^2 + s^2 = 1$, we can find analytical solutions for Z_N , Z_V , and ϕ . We obtain

$$Z_N = \frac{s_{11} - s_{22}}{s^2} + \frac{s_{13} - s_{23}}{s^2} = \frac{s_{15} + s_{35}}{2cs}, \quad (83)$$

$$Z_V = \frac{s_{11} - s_{22}}{s^2} - \frac{s_{13} - s_{23}}{c^2} = \frac{c^2 s_{15} - s^2 s_{35}}{cs(c^2 - s^2)}, \quad (84)$$

and

$$\frac{s}{c} = \tan \phi = 2 \frac{(s_{11} - s_{22}) + (s_{13} - s_{23})}{s_{15} + s_{35}}, \quad -\frac{\pi}{2} < \phi < \frac{\pi}{2}. \quad (85)$$

We also obtain the constraint $\Omega_1 = 0$, where the dimensionless quantity Ω_1 is defined by

$$\Omega_1 = \tan \phi - \frac{1}{\tan \phi} - \frac{1}{2} \frac{s_{15} - s_{35}}{s_{13} - s_{23}} = 0. \quad (86)$$

Transversely isotropic symmetry also demands that $s_{46_b} = 0$, which allows us to solve for the remaining unknown, Z_H . We obtain

$$Z_H = \frac{s_{46}}{cs}. \quad (87)$$

The first condition of equation (82), $s_{44_b} = s_{55_b}$, allows us to define a second constraint, $\Omega_2 = 0$, where

$$\Omega_2 = (s_{55} - s_{44}) \tan \phi + s_{46} - \tan^2 \phi s_{35} - s_{15} = 0. \quad (88)$$

The condition, $s_{12_b} = s_{11_b} - \frac{1}{2}s_{66_b}$, of (82) allows us to define a third constraint, $\Omega_3 = 0$, where

$$\Omega_3 = \tan \phi + \frac{2(s_{22} - s_{12}) - s_{66}}{s_{46}} = 0. \quad (89)$$

How close the dimensionless quantities Ω_i actually approach zero is a useful test of the model and a measure of the quality of the inversion.

A fracture system displaying hexagonal symmetry is axisymmetric, i.e., $Z_V \equiv Z_H$, which provides an additional constraint, $\Omega_4 = 0$. If the background is isotropic, the three additional conditions

$$s_{22_b} = s_{33_b}, \quad s_{12_b} = s_{13_b}, \quad s_{55_b} = s_{66_b} \quad (90)$$

force three more non-dimensional quantities, Ω_5 , Ω_6 , and Ω_7 , to equal zero. These relationships constrain the inversion for the background and fracture systems.

The process outlined above defines the fracture compliances and ϕ as functions of the measured parameters. The fracture compliances, Z_N , Z_V , Z_H , and the fracture dip angle ϕ may then be substituted back into \mathbf{S}_b . This gives the background moduli in terms of the measured s_{ij} of \mathbf{S} and completes the inversion for all the unknown parameters.

Discussion

The foregoing method derives explicit formulae for the fracture compliances, fracture orientation, and the background elastic moduli. These formulae are functions of the measured moduli of the long wavelength equivalent medium.

Once elastic moduli are obtained, the fracture dip angle and the complexity of the background symmetry can be determined. Assuming a particular background symmetry, implies a set of relationships the measured moduli s_{ij} must satisfy. For example, specific relationships among the measured moduli result, namely, for a transversely isotropic background equations (86), (88), and (89) must hold. These provide the bases for determining how closely the subject medium conforms to the specified symmetry. The dimensionless quantity

$$\Phi = \sum_i \Omega_i^2 \tag{91}$$

will be a useful measure of how well the model fits the data. If (91) is suitably small, these calculations will estimate the fracture dip angle, the relevant fracture compliances, and the moduli of the unfractured background.

CONCLUSIONS

The foregoing methods can be used to determine whether a medium results from fractures embedded in an anisotropic background. The interdependences among some of the elastic parameters provide bases for determining how closely the subject medium conforms to the model. If they do, these calculations determine the relevant fracture compliances, the fracture orientation, and the moduli of the background without these fractures. Specific relationships among the measured moduli constrain the symmetry of the background medium. Additional relations on the measured moduli may hold and would constrain the fracture behavior.

If the azimuthal anisotropy is believed to be caused by parallel long wavelength fractures, then each fracture compliance corresponds to the ratio of the displacement discontinuity across a typical fracture per corresponding unit stress to the mean spacing between the fractures. If it is assumed to be caused by aligned flat ellipsoidal microcracks [Hudson, 1981], the δ of equation (9) are related to the product of the crack density and a parameter that depends on the elastic properties of the background and the nature and properties of the infilling material. For circular, axially symmetric cracks, this dimensionless crack density e is defined as the number of cracks per a volume given by the mean crack radius cubed. Hence e may be written

$$e = 3\phi_c/4\pi\alpha, \quad (92)$$

where ϕ_c is the crack porosity and α is the mean aspect ratio of the flat ellipsoidal inclusions [Schoenberg and Douma, 1988]. Since the parameter separation method does not differentiate between long parallel fractures and aligned microcracks, it is applicable to either model.

APPENDIX

Outline of the Schoenberg and Muir Calculus

Hooke's law for a general linear elastic medium in condensed notation [Auld, 1973]

is

$$\begin{bmatrix} \sigma_1 \\ \sigma_2 \\ \sigma_3 \\ \sigma_4 \\ \sigma_5 \\ \sigma_6 \end{bmatrix} = \begin{bmatrix} c_{11} & c_{12} & c_{13} & c_{14} & c_{15} & c_{16} \\ c_{12} & c_{22} & c_{23} & c_{24} & c_{25} & c_{26} \\ c_{13} & c_{23} & c_{33} & c_{34} & c_{35} & c_{36} \\ c_{14} & c_{24} & c_{34} & c_{44} & c_{45} & c_{46} \\ c_{15} & c_{25} & c_{35} & c_{45} & c_{55} & c_{56} \\ c_{16} & c_{26} & c_{36} & c_{46} & c_{56} & c_{66} \end{bmatrix} \begin{bmatrix} \epsilon_1 \\ \epsilon_2 \\ \epsilon_3 \\ \epsilon_4 \\ \epsilon_5 \\ \epsilon_6 \end{bmatrix} \quad (\text{A1})$$

where the stress components are defined as

$$[\sigma_1, \sigma_2, \sigma_3, \sigma_4, \sigma_5, \sigma_6]^t \equiv [\sigma_{11}, \sigma_{22}, \sigma_{33}, \sigma_{23}, \sigma_{13}, \sigma_{12}]^t \quad (\text{A2})$$

and the strain components are defined as

$$[\epsilon_1, \epsilon_2, \epsilon_3, \epsilon_4, \epsilon_5, \epsilon_6]^t \equiv [\epsilon_{11}, \epsilon_{22}, \epsilon_{33}, 2\epsilon_{23}, 2\epsilon_{13}, 2\epsilon_{12}]^t . \quad (\text{A3})$$

The σ_{ij} and ϵ_{ij} are elements of the stress and strain tensors, respectively. Superscript t denotes the transpose. These six equations can be written in a form that decomposes internal and external stress and strain components relative to a specified preferred direction. Schoenberg and Muir [1989] considered layered media with the x_3 axis normal to the layering, and thus defined the external stress and strain components

relative to that axis. No essential changes result from assuming that this layering is normal to any other coordinate axis, however, when this method is applied to vertical fractures, it is natural to call the horizontal normal to the layering the x_1 axis and decompose relative to that direction. The external stress and strain components contain the subscript 1 in the full notation (i.e., terms with subscripts 1, 5, and 6 in condensed notation) and are denoted by N for normal. The internal components, those not containing subscripts 1 in the full notation, are denoted by T for tangential (i.e., terms with subscripts 2, 3, and 4). In other words, external components are $11 \rightarrow 1$, $13 \rightarrow 5$, and $12 \rightarrow 6$ and internal components are $22 \rightarrow 2$, $33 \rightarrow 3$, and $23 \rightarrow 4$. The stress-strain relations (A1) can now be rewritten as

$$\begin{bmatrix} \sigma_1 \\ \sigma_5 \\ \sigma_6 \end{bmatrix} = \mathbf{C}_{NN} \begin{bmatrix} \epsilon_1 \\ \epsilon_5 \\ \epsilon_6 \end{bmatrix} + \mathbf{C}_{NT} \begin{bmatrix} \epsilon_2 \\ \epsilon_3 \\ \epsilon_4 \end{bmatrix} \quad (\text{A4})$$

$$\begin{bmatrix} \sigma_2 \\ \sigma_3 \\ \sigma_4 \end{bmatrix} = \mathbf{C}_{TN} \begin{bmatrix} \epsilon_1 \\ \epsilon_5 \\ \epsilon_6 \end{bmatrix} + \mathbf{C}_{TT} \begin{bmatrix} \epsilon_2 \\ \epsilon_3 \\ \epsilon_4 \end{bmatrix}$$

with

$$\begin{aligned} \mathbf{C}_{NN} &= \begin{bmatrix} c_{11} & c_{15} & c_{16} \\ c_{15} & c_{55} & c_{56} \\ c_{16} & c_{56} & c_{66} \end{bmatrix}, \\ \mathbf{C}_{TN} &= \begin{bmatrix} c_{12} & c_{25} & c_{26} \\ c_{13} & c_{35} & c_{36} \\ c_{14} & c_{45} & c_{46} \end{bmatrix}, \quad \mathbf{C}_{NT} = \mathbf{C}_{TN}^t, \\ \mathbf{C}_{TT} &= \begin{bmatrix} c_{22} & c_{23} & c_{24} \\ c_{23} & c_{33} & c_{34} \\ c_{24} & c_{34} & c_{44} \end{bmatrix}. \end{aligned} \quad (\text{A5})$$

The subscripts NN , TN , NT , and TT describe the components of stress and strain to which the submatrices refer. NN relates stress and strain components acting on the plane normal to x_1 (i.e., the 1, 5, 6 components); TN relates stress components acting in the plane normal to x_1 (i.e., the 2, 3, 4 components) to the normal strain components; NT , indicating the transpose of the corresponding TN

submatrix, relates normal stress components to tangential strain components; and TT relates tangential stress components to tangential strain components. Note that C_{NN} and C_{TT} are symmetric.

A layered medium composed of several constituent media, each in general anisotropic, is elastodynamically identical to an equivalent homogeneous anisotropic medium if the layered medium is statistically stationary over any sample of layering as thick or thicker than the shortest wavelength [Backus, 1962]. The information required to determine the properties of the equivalent medium are density, elastic moduli, and the concentration of each constituent.

Consider a region of thickness H composed of layers with welded interfaces where the x_1 axis is perpendicular to the layering. The total thickness of all layers of the i th constituent is H times the concentration of that constituent. Let this total thickness be H_i , the density be ρ_i , and the three elastic moduli submatrices be C_{NN_i} , C_{TN_i} , and C_{TT_i} according to (A5). The quantities H_i , ρ_i , C_{NN_i} , C_{TN_i} , and C_{TT_i} are the physical model parameters of the i th constituent. These physical model parameters map into a 5-vector \mathbf{G}_i , consisting of scalars and 3×3 matrices. The first two components of \mathbf{G}_i are scalars and the third, fourth and fifth components are 3×3 matrices. The third and fifth are symmetric. The mapping is

$$\begin{bmatrix} H_i \\ \rho_i \\ C_{NN_i} \\ C_{TN_i} \\ C_{TT_i} \end{bmatrix} \rightarrow \begin{bmatrix} H_i \\ H_i \rho_i \\ H_i C_{NN_i}^{-1} \\ H_i C_{TN_i} C_{NN_i}^{-1} \\ H_i [C_{TT_i} - C_{TN_i} C_{NN_i}^{-1} C_{TN_i}^t] \end{bmatrix} = \begin{bmatrix} g_i(1) \\ g_i(2) \\ \mathbf{g}_i(3) \\ \mathbf{g}_i(4) \\ \mathbf{g}_i(5) \end{bmatrix} = \mathbf{G}_i. \quad (\text{A6})$$

For any \mathbf{G}_i with $g_i(1) \neq 0$ and $\mathbf{g}_i(3)$ invertible, the set of physical model parameters are returned by the inverse mapping:

$$\mathbf{G}_i \rightarrow \begin{bmatrix} g_i(1) \\ g_i(2)/g_i(1) \\ g_i(1)\mathbf{g}_i(3)^{-1} \\ \mathbf{g}_i(4)\mathbf{g}_i(3)^{-1} \\ [\mathbf{g}_i(5) + \mathbf{g}_i(4)\mathbf{g}_i(3)^{-1}\mathbf{g}_i(4)^t]/g_i(1) \end{bmatrix} = \begin{bmatrix} H_i \\ \rho_i \\ C_{NN_i} \\ C_{TN_i} \\ C_{TT_i} \end{bmatrix}. \quad (\text{A7})$$

This formulation is powerful because the 5-vector \mathbf{G} of the homogeneous medium equivalent to a layered medium composed of n constituents is simply the sum of the

5-vectors of the n constituent media, i.e.,

$$\mathbf{G} = \sum_{i=1}^n \mathbf{G}_i . \quad (\text{A8})$$

In the domain of these 5-vectors, addition corresponds to combining layers. The set of physical model parameters of the equivalent medium is found by applying the inverse mapping (A7) to \mathbf{G} .

REFERENCES

- Alford, R. M., 1986, Shear data in the presence of azimuthal anisotropy: Dilley, Texas, *Expanded Abstracts, 56th Ann. Int'l. SEG Meeting, Houston*, 476–479.
- Auld, B. A., 1973, *Acoustic Fields and Waves in Solids*, John Wiley & Sons, New York.
- Backus, G. E., 1962, Long-wave anisotropy produced by horizontal layering, *J. Geophys. Res.*, **66**, 4,427–4,440.
- Crampin, S., 1985, Evaluation of anisotropy by shear-wave splitting, *Geophysics*, **50**, 142–152.
- Fryer, G. J., D. J. Miller, and P. A. Berge, 1990, Seismic anisotropy and age-dependent structure of the upper oceanic crust, in *The Evolution of Mid-Oceanic Ridges*, edited by J. M. Sinton, AGU, Washington, D.C., in press.
- Garbin, H. D., and L. Knopoff, 1973, The compressional modulus of a material permeated by a random distribution of circular cracks, *Q. Appl. Math.*, **30**, 453–464.
- Garbin, H. D., and L. Knopoff, 1975, The shear modulus of a material permeated by a random distribution of free circular cracks, *Q. Appl. Math.*, **33**, 296–300.
- Hoening, A., 1978, The behaviour of a flat elliptical crack in an anisotropic elastic body, *Int. J. Solids Structures*, **14**, 925–934.
- Hoening, A., 1979, Elastic moduli of a non-randomly cracked body, *Int. J. Solids Structures*, **15**, 137–154.
- Hubbert, M. K. and D. G. Willis, 1957, Mechanics of hydraulic fracturing, *Trans. AIME*, **210**, 153–170.
- Hudson, J. A., 1980, Overall properties of a cracked solid, *Math. Proc. Camb phil. Soc.*, **88**, 371–384.

- Hudson, J. A., 1981, Wave speeds and attenuation of elastic waves in material containing cracks, *Geophys. J. R. Astr. Soc.*, **64**, 133–150.
- Newmark, R. L. , R. N. Anderson, D. Moos, and M. D. Zoback, 1985, Sonic and ultrasonic logging of Hole 504B and its implications for the structure, porosity, and stress regime of the upper 1 km of the oceanic crust, *Initial Reports from the Deep Sea Drilling Project*, **83**, 479–510.
- Nichols, D., F. Muir, and M. Schoenberg, 1989, Elastic properties of rocks with multiple sets of fractures, *Expanded Abstracts, 59th Ann. Int'l. SEG Meeting, Dallas*, 471–474
- Postma, G. W., 1955, Wave propagation in a stratified medium, *Geophysics*, **20**, 780–806.
- Schoenberg, M., 1980, Elastic wave behavior across linear slip interfaces, *J. Acoust. Soc. Am.*, **68**, 1,516–1,521.
- Schoenberg, M., 1983, Reflection of elastic waves from periodically stratified media with interfacial slip, *Geophys. Prosp.*, **31**, 265–292.
- Schoenberg, M. and J. Douma, 1988, Elastic wave propagation in media with parallel fractures and aligned cracks, *Geophys. Prosp.*, **36**, 571–590.
- Schoenberg, M. and F. Muir, 1989, A calculus for finely layered anisotropic media, *Geophysics*, **54**, 581–589.
- Stephen, R. A., 1985, Seismic anisotropy in the upper oceanic crust, *J. Geophys. Res.*, **90**, 11,383–11,396.
- Willis, H. A., G. L. Rethford, E. Bielanski, 1986, Azimuthal anisotropy: occurrence and effect on shear-wave data quality, *Expanded Abstracts, 56th Ann. Int'l. SEG Meeting, Houston*, 479–481.